
Self-Supervised Animal Identification for Long Videos

Xuyang Fang, Sion Hannuna, Edwin Simpson, Neill Campbell

University of Bristol

{xf16910, sh1670, Neill.Campbell, edwin.simpson}@bristol.ac.uk

Abstract

Identifying individual animals in long-duration videos is essential for behavioral ecology, wildlife monitoring, and livestock management. Traditional methods require extensive manual annotation, while existing self-supervised approaches are computationally demanding and ill-suited for long sequences due to memory constraints and temporal error propagation. We introduce a highly efficient, self-supervised method that reframes animal identification as a global clustering task rather than a sequential tracking problem. Our approach assumes a known, fixed number of individuals within a single video—a common scenario in practice—and requires only bounding box detections and the total count. By sampling pairs of frames, using a frozen pre-trained backbone, and employing a self-bootstrapping mechanism with the Hungarian algorithm for in-batch pseudo-label assignment, our method learns discriminative features without identity labels. We adapt a Binary Cross Entropy loss from vision-language models, enabling state-of-the-art accuracy (>97%) while consuming less than 1 GB of GPU memory per batch—an order of magnitude less than standard contrastive methods. Evaluated on challenging real-world datasets (3D-POP pigeons and 8-calves feeding videos), our framework matches or surpasses supervised baselines trained on over 1,000 labeled frames, effectively removing the manual annotation bottleneck. This work enables practical, high-accuracy animal identification on consumer-grade hardware, with broad applicability in resource-constrained research settings. All code written for this paper are here.

1 Introduction

Identifying individual animals across long-duration video sequences is a fundamental challenge in behavioral ecology, wildlife monitoring, and livestock management. The ability to consistently recognize individuals without manual intervention enables researchers to track behavior, social interactions, and health over time, providing critical insights into animal welfare and population dynamics. Traditional approaches often rely on supervised learning, which requires extensive manual annotation of identity labels—a tedious, costly, and often impractical process for large video datasets. While recent advances in self-supervised learning offer promising alternatives by learning representations without explicit labels, these methods are typically designed for general-purpose visual representation learning and are ill-suited to the specific constraints of animal identification in long videos.

Two primary challenges hinder the application of existing self-supervised frameworks to this domain. First, computational and memory constraints limit scalability: methods such as SimCLR and MoCo require large batch sizes or memory banks to learn effective representations, often consuming over 10GB of GPU memory per batch—a prohibitive requirement for many research settings. Second, temporal error propagation plagues sequential tracking paradigms: even state-of-the-art tracking methods (e.g., 3D-MuPPET) rely on frame-by-frame association, where a single identity switch can propagate indefinitely in long sequences, degrading performance over time. These limitations

are particularly acute in videos lasting hours or days, where manual correction is infeasible and computational resources are often constrained.

Our work addresses a specific but common and valuable scenario: the identification of a known, fixed number of individual animals within a single video. This assumption holds true in many practical settings, such as monitoring a defined group of livestock in a pen, a specific colony of laboratory animals, or a set number of birds at a feeder. Under this assumption, we reframe the animal identification problem as a global clustering task rather than a sequential tracking problem. We introduce a resource-efficient, self-supervised method that learns to distinguish individuals without any identity labels, relying only on pre-existing bounding box detections and the prior knowledge of the total count of distinct individuals.

Our approach samples pairs of frames from a video, extracts animal crops, and applies augmentations to create multiple views. Using a pre-trained backbone network, we compute feature vectors and construct a similarity matrix across all augmented instances. We used the Hungarian algorithm within each training batch to dynamically assign positive pairs based on feature similarity, effectively generating pseudo-labels that guide representation learning. This self-bootstrapping mechanism allows the network to learn discriminative features specific to the fixed set of animal identities, even when initialized with generic pre-trained weights. After training, a single pass over all video frames produces feature embeddings that are clustered using K-Means, with the number of clusters set to the known population size.

Designed with minimal memory consumption as a core objective, our method samples only two frames per batch, allows for a frozen backbone, and employs efficient loss functions—including a Binary Cross Entropy (BCE) loss adapted from vision-language models like SigLIP[1]. This reduces memory usage to below 1GB per batch while achieving state-of-the-art accuracy. We evaluate our approach on challenging real-world datasets, including the 3D-POP pigeon dataset and an 8-calves feeding video, demonstrating robust performance (>97% accuracy) that matches or exceeds supervised baselines trained on over 1,000 labeled frames.

While our approach shares the use of random frame sampling and the Hungarian algorithm for in-batch pseudo-label assignment with recent multi-object tracking work[2], our key contributions lie in the specific design choices that enable high efficiency and applicability to single-video animal identification:

1. **Single-video, single-species optimization:** Unlike methods that sample from multiple videos to maximize negative diversity, we sample frames solely from the target video. This reduces computational overhead and memory footprint while being sufficient for learning discriminative features within a closed population.
2. **Frozen backbone compatibility:** Our method functions effectively even when the feature extraction backbone is frozen, requiring only a lightweight projection head to be trained. This reduces memory usage by approximately 60% while maintaining high accuracy, leveraging the transfer learning capabilities of pre-trained models.
3. **Minimalist loss formulation:** We demonstrate that a single loss function—either a Supervised Contrastive Loss or, more effectively, a Binary Cross Entropy loss adapted from vision-language models—is sufficient for this task. This simplifies the hyperparameter search and reduces computational complexity compared to multi-loss frameworks.
4. **High memory efficiency:** Through strategic batch construction (sampling only 2 frames), optimized augmentation strategies, and the aforementioned design choices, we achieve state-of-the-art accuracy with a memory footprint of less than 1GB—an order of magnitude less than standard contrastive methods.

The remainder of this paper is structured as follows: Section 2 details our method, including batch construction, similarity computation, masking, and loss functions. Section 3 describes experimental setups, datasets, and baselines. Section 4 presents results and comparisons with state-of-the-art methods. Section 5 discusses related work, and Section 6 concludes with future directions.

2 Method

Our method is applied to video datasets of animals of the same type where the bounding boxes of each animal have already been extracted.

2.1 Training Loop

The schematic diagram of the training loop of our self-supervised method is displayed in Figure 1.

2.1.1 Construct a training batch

To construct a training batch, we randomly select a user-defined number of frames, K (where $K \geq 2$), denoted as $\{F_1, F_2, \dots, F_K\}$. While generalised for K frames, setting $K = 2$ minimises the memory needed for training. Our diagram is a special case where $K = 3$. We then crop the corresponding bounding boxes to each frame. Each cropped image then gets augmented twice, which doubles the number of images in the batch.

2.1.2 Compute the Similarity Matrix

After the batch is constructed, it gets passed through a neural network, which converts each image to a high-dimensional feature vector. The batch of feature vectors is shown in Figure 1 as coloured blocks. The colours that contain the same combination of primary colours (e.g., purple and pink) indicate those two blocks represent two instances of augmentations applied to cropped images from the same frame. We then compute the similarity score for each and every other vector within the batch. The diagonal elements of the similarity matrix record the self-similarity for each vector.

2.1.3 Construct the Mask for the Similarity Matrix

The mask matrix has exactly the same size as the similarity matrix. Colour red, green and white denote the similarity scores that should be discarded, maximised and minimised.

The matrix is organized into four quadrants representing the similarity between the two augmented views (Instance 1 and Instance 2). As shown in Figure 1, the diagonal quadrants (Top-Left, Bottom-Right) represent intra-view similarities, while off-diagonal quadrants represent inter-view similarities.

We then divide each quadrant into submatrices such that each submatrix contains the similarity score of feature vectors originated from each frame. Each off-diagonal submatrix contains the similarity score between feature vectors originated from different frames. Each diagonal submatrix contains the similarity score between feature vectors originated from the same frames. We discard the diagonal elements of the top-left and bottom-right quadrants since they record the self-similarity score of each feature vector originated from the same augmented instance. However, we mark the diagonal elements of the bottom-left and top-right quadrants as green, since they record the self-similarity score of each feature vector originated from different augmented instances. To determine the mask for off-diagonal submatrices, we employ a heuristic based on the assumption that the network—initialized with a pre-trained backbone—is capable of extracting meaningful features from the outset. Consequently, we treat the optimal assignment of pairs (the permutation that maximizes total similarity) as a proxy for ground truth. We apply the Hungarian Algorithm to each off-diagonal submatrix to identify these positive pairs. This process allows the network to self-bootstrap: the pre-trained features guide the initial masking, which in turn supervises the network to learn more discriminative representations specific to the animal identities.

2.1.4 Loss Function

We feed both the similarity matrix and the mask to the loss function. The choice of the loss function could either be a Supervised Contrastive Loss, where the total loss, $\mathcal{L}_{\text{SupCon}}$, is the average of the loss of each positive in the row of each similarity matrix (as Equation 1 shows):

$$\mathcal{L}_{\text{SupCon}} = \frac{1}{|\mathcal{P}|} \sum_{(i,j) \in \mathcal{P}} \mathcal{L}_{i,j} \quad (1)$$

Where \mathcal{P} denotes the set of matrix index pairs that are marked by colour green in the corresponding mask (as Figure 1 shows), and i and j denote the row and column numbers respectively. The loss of each positive is described by Equation 2:

$$\mathcal{L}_{i,j} = -\log \frac{\exp(\mathbf{Sim}_{i,j}/\tau)}{\sum_{k \in \{1:N\}, k \neq i} \exp(\mathbf{Sim}_{i,k}/\tau)} \quad (2)$$

Where \mathbf{Sim} is the similarity matrix, N is the size of the similarity matrix, τ is a temperature parameter that can either be arbitrarily set by the user to a constant or a learnable parameter and k is the column number. $k \neq i$ indicates that the diagonals marked as red ($i \neq j$) in Figure 1 are discarded.

The loss could also be the Binary Cross Entropy Loss, where the total loss, \mathcal{L}_{BCE} , is computed as

$$\mathcal{L}_{\text{BCE}} = -\frac{1}{N^2} \sum_{i,j \in \{1:N, 1:N\}, i \neq j} \log \sigma\left(M_{ij} \frac{\mathbf{Sim}_{i,j}}{\tau}\right) \quad (3)$$

Where σ is the sigmoid function and M is the mask matrix in Figure 1 where colour green indicates $M_{ij} = 1$ and colour white indicates $M_{ij} = -1$. Like the SupCon loss, the diagonals marked as red are discarded. While τ can be treated as a fixed hyperparameter, we treat it as a learnable parameter to improve training stability. Following the strategy in SigLIP[1], we parameterize the logit scaling as $\mathbf{Sim}_{i,j} \cdot t + b$, where t and b are learnable scalars initialized to 10 and -10. We clamped the value of t between 0 – 100.

2.1.5 Updating the Network

Once the loss is computed, we use backpropagation to compute the gradient, then use SGD with momentum to update the network.

2.2 Inference

Once the network is trained, we convert all images from the dataset to feature vectors by forward passing them through the network. We then use the KMeans algorithm to group the vectors into N_{ID} clusters, where N_{ID} corresponds to the known number of distinct animal identities in the video. Throughout the entire training and inference process, no ground truth identity of each cropped image is used.

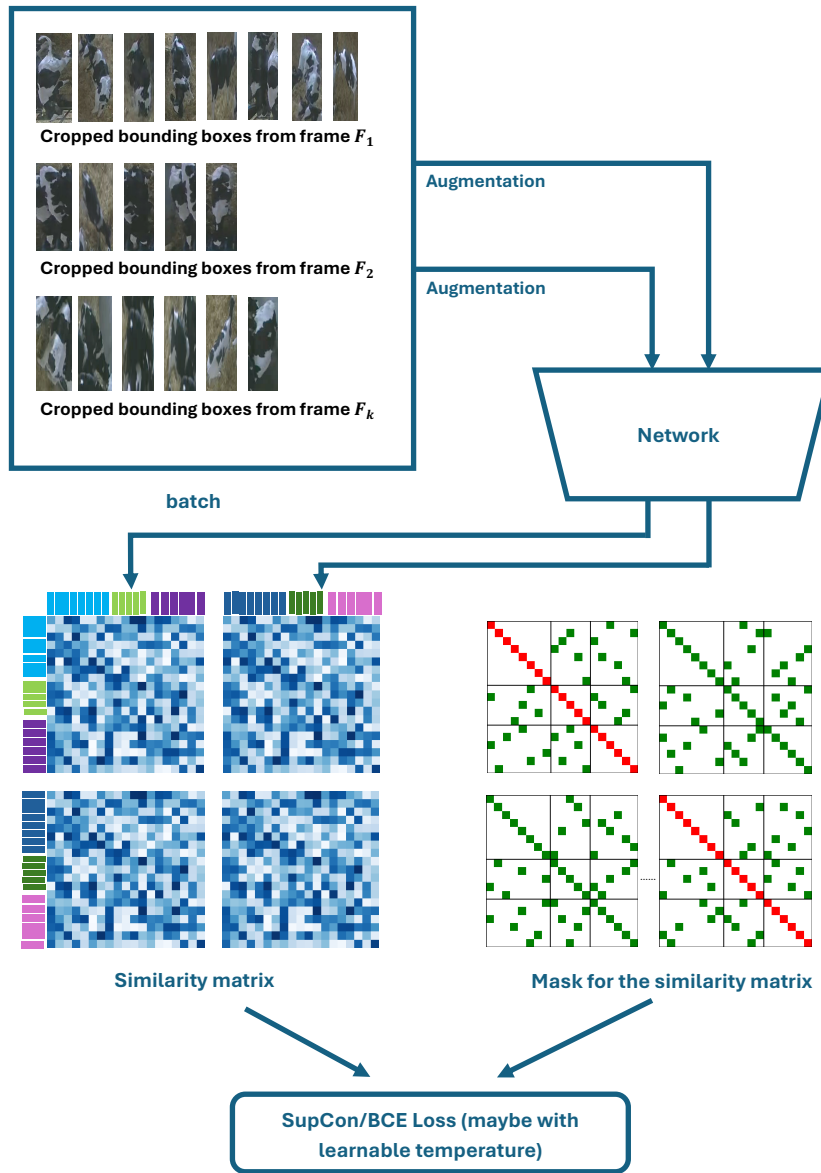


Figure 1: Schematic Diagram of the training pipeline of our method.

3 Experimental Details

3.1 Choice of Datasets

We applied our method to datasets constructed from 3 separate videos. One is the 8-Calves dataset, constructed from a 1-hr video of 8 calves feeding in a barn. The other two are selected from the 59 videos in the 3D-POP[3] dataset that records the feeding of 18 pigeons on different days. To maximise the robustness of our method, we selected the two videos containing the highest number of pigeons (10) while sharing the fewest common identities (4). These videos were recorded by different cameras on different days, ensuring the visual data is as distinct as possible. This selection strategy evaluates whether our method generalizes to videos taken from different camera angles on different days that record a different set of individuals. The specific sequences used were Sequence11_n10_01072022-Cam2 and Sequence19_n10_13072022-Cam4 (hereafter referred to as Seq11 and Seq19). We used the pre-existing bounding boxes provided by these datasets to crop the frames and constructed 3 image datasets.

3.2 Network Design

We want to use a network where the GPU memory consumption during training is minimal. We tested 2 network setups. The first setup contains a pre-trained backbone with its classification module replaced by a linear layer with an output size of 64. Every parameter in this network is trainable. The second setup contains a frozen pre-trained network with an MLP that has the following structure:

- Linear(backbone_output_size, 256) + BatchNorm1d + ReLU
- Linear(256, 128) + BatchNorm1d + ReLU
- Linear(128, 128) + BatchNorm1d + ReLU
- Linear(128, 64)

For the first setup, we limit the choice of backbone to ResNet18 and EfficientNet-B0; we specifically avoided training transformer backbones to avoid the high memory overhead associated with attention mechanisms. For the 2nd setup, we expanded the choice of backbone to ConvNextV2, since the backbone would be frozen. Implementation-wise, all methods were developed using PyTorch. We utilized pre-trained weights from the `torchvision` library for ResNet18 and EfficientNet-B0, while ConvNextV2 weights were sourced from Hugging Face.

3.3 Training Details

Augmentation: We applied two augmentations to double the size of our batch. They are random horizontal flip and random resized crop to images with a size of (224, 224) and a scale of (0.2, 1.0). Unlike standard contrastive learning approaches such as simCLR[4] and MoCo[5], we did not apply color jitter or Gaussian blur.

Sampling Strategy (Batch Size): To minimise GPU memory consumption, we constructed each training batch by randomly sampling $K = 2$ frames from the video. Since the number of visible bounding boxes varies due to occlusion or detection failures, the effective batch size is dynamic. For a video with a maximum of 10 individuals, the effective batch size is ≤ 40 image crops per iteration ($K = 2 \times 10 \text{ max animals} \times 2 \text{ augmented views}$).

Loss Function: We tested 3 loss functions: BCE with a learnable temperature (as Equation 3 shows), SupCon with a fixed temperature, 0.5, and SupCon with a learnable temperature. For the SupCon with a learnable temperature, we replaced $1/\tau$ in Equation 2 with a weight, t . Followed the strategy of CLIP[6], we clamped the value of t between 0 – 100 and set its initial value to 14.

Optimiser Settings: We used SGD to update the network weights of our method. We set momentum to 0.9, weight decay to 0 and an initial learning rate to $0.3 \times \text{batchsize}/256$. We also used a cosine annealing scheduler to alter the learning rate during training.

3.4 Inference Details

We used KMeans to group the vectors into clusters. Then to calculate the accuracy of our method, we optimally matched the clusters with the ground truth identities via the Hungarian Algorithm.

3.5 Baselines for Comparison

To evaluate the effectiveness of our approach against standard contrastive learning baselines, we compared our method against supervised and self-supervised methods. We implemented all methods in PyTorch using a ResNet18 backbone.

For self-supervised methods, we tested SimCLR[4] and MoCo[5]. For MoCo, the momentum encoder was also a ResNet18 instance with gradient updates disabled. For MoCo, we utilized a momentum value of $m = 0.999$ and a memory bank size 32 times of the batch size. Crucially, to test the feasibility of these methods on the same resource-constrained hardware targeted by our approach, we limited their batch size to 256. While these methods typically utilize larger batches, this constraint allows for a direct comparison of resource efficiency. We kept the Optimiser settings for these two methods identical to our own.

For the supervised approach, the network architecture, hyperparameters and batch construction were all kept the same as our own method. The key distinctions are that, (1) the dataset was split into train, validation and test sets; (2) During training, no similarity matrix is computed. The ground truths were directly used to compute the Cross Entropy Loss. We also employed an early stopping condition based on the validation loss with patience of 10 epochs to prevent overfitting.

4 Results

4.1 Comparison with simCLR and MoCo

While standard contrastive methods like SimCLR and MoCo are powerful, our results demonstrate they are inefficient for this specific domain. As shown in Table 1, these methods require over 10GB of memory per batch yet fail to achieve meaningful accuracy ($\sim 30\%$).

Conversely, our method achieves state-of-the-art accuracy ($>97\%$) with a memory footprint of less than 1GB. This efficiency offers a dual advantage:

1. Accessibility: It enables deployment on lower-end hardware.
2. Scalability: Even on a high-end GPU, our method frees up GPU memory, providing users the options to run other computational tasks on the same GPU concurrently.

4.2 Comparison with the SOTA on 3D-POP and 8-Calves

While 3D-MuPPET achieves state-of-the-art performance on the 3D-POP dataset (0.96 ID-F1), it relies on a sequential tracking paradigm (using SORT on extracted keypoints). A fundamental limitation of sequential trackers is error propagation: a single identity switch can persist indefinitely, requiring manual intervention to correct. This limitation becomes acute in long-duration footage. For instance, when applying standard tracking baselines (ByteTrack/Bot-SORT on bounding boxes) to the 1-hour 8-Calves dataset, we observed a performance drop to an ID-F1 of approximately 0.15.

In contrast, our method treats identification as a global clustering problem rather than a sequential tracking problem. By grouping feature vectors from the entire video simultaneously (as described in the Method Section), our approach eliminates the dependency on previous frames, thereby preventing error propagation. This allows our method to maintain high accuracy ($> 90\%$) on long-duration videos where sequential trackers fail.

4.3 Comparison with Supervised Baselines

Remarkably, our self-supervised method (using BCE) matches or exceeds the performance of the supervised baseline trained on 1,000 labeled frames. For example, on the 3D-POP Sequence19 dataset, the supervised baseline achieves 97% accuracy only after training on 1,000 frames. In

contrast, our method achieves 99.8% accuracy without utilizing any ground-truth identity labels during training. This highlights a significant practical advantage: to replicate the performance of our self-supervised pipeline using a standard supervised approach, a user would be required to manually annotate at least 1,200 frames (1,000 for training and 200 for validation). Our method eliminates this manual bottleneck entirely while maintaining state-of-the-art accuracy.

4.4 Ablation Studies on our method

4.4.1 Comparison of Loss functions

We evaluated the impact of the loss function on model performance. As shown in Tables tables 1 to 3, the Binary Cross Entropy (BCE) loss consistently outperforms or matches the Supervised Contrastive (SupCon) loss. For instance, on Sequence 11, BCE achieves an accuracy of 97.6% compared to 92.6% for SupCon with a fixed temperature. While introducing a learnable temperature to SupCon closes this gap, BCE remains the most robust and stable choice across all datasets without requiring additional hyperparameter tuning.

4.4.2 Memory Usage vs Accuracy

To further investigate the lower bound of GPU memory consumption during training, we experimented with freezing the backbone and training only the projection MLP. This strategy yields significant memory savings. For ResNet18, freezing the backbone reduces memory usage by approximately 60% (from 1.04 GB to 0.42 GB). Despite this massive reduction in computational cost, the model retains strong performance, achieving between 86–90% accuracy across datasets. This confirms that a pre-trained ImageNet backbone extracts sufficiently discriminative features for animal identification, allowing for extremely lightweight adaptation.

4.4.3 Backbone Architecture Analysis

We also analyzed the choice of backbone architecture. Contrary to expectations, EfficientNet-B0 proved less memory-efficient than ResNet18 for our specific training setup. Despite having fewer parameters, EfficientNet-B0 requires storing significantly more activations during the forward pass due to its depth, resulting in a memory footprint of 3.44 GB per batch compared to 1.04 GB for ResNet18. Consequently, ResNet18 remains the optimal choice for minimizing peak memory usage.

| Loss | Network | Train MLP Only | Memory Per Batch (GB) | Accuracy |
|---------|-----------------|-------------------|--------------------------|-------------------|
| BCE | ResNet18 | False | 1.044 ± 0.000 | 0.976 ± 0.021 |
| BCE | ResNet18 | True | 0.418 ± 0.000 | 0.866 ± 0.008 |
| BCE | ConvNextV2 | True | 0.696 ± 0.000 | 0.899 ± 0.003 |
| BCE | EfficientNet-B0 | False | 3.440 ± 0.001 | 0.980 ± 0.011 |
| BCE | EfficientNet-B0 | True | 0.521 ± 0.000 | 0.897 ± 0.079 |
| Supcon | ResNet18 | False | 1.044 ± 0.000 | 0.926 ± 0.036 |
| Supcon | ResNet18 | True | 0.418 ± 0.000 | 0.643 ± 0.047 |
| Supcon | ConvNextV2 | True | 0.696 ± 0.000 | 0.740 ± 0.070 |
| Supcon* | ResNet18 | False | 1.044 ± 0.000 | 0.977 ± 0.012 |
| Supcon* | ResNet18 | True | 0.418 ± 0.000 | 0.736 ± 0.008 |
| Supcon* | ConvNextV2 | True | 0.696 ± 0.000 | 0.715 ± 0.066 |
| MoCo | ResNet18 | False | 7.369 ± 0.003 | 0.278 ± 0.028 |
| SimCLR | ResNet18 | False | 10.867 ± 0.004 | 0.312 ± 0.050 |

Table 1: 3D-POP Sequence11 Epoch 10. The asterisk (*) indicates models trained using Supcon with learnable temperature.

| Loss | Network | Train MLP Only | Memory Per Batch (GB) | Accuracy |
|---------------------|-----------------|-------------------|--------------------------|-------------------|
| BCE | ResNet18 | False | 1.044 \pm 0.000 | 0.998 \pm 0.000 |
| BCE | ResNet18 | True | 0.418 \pm 0.000 | 0.898 \pm 0.089 |
| BCE | ConvNextV2 | True | 0.696 \pm 0.000 | 0.847 \pm 0.052 |
| BCE | EfficientNet-B0 | False | 3.441 \pm 0.000 | 0.993 \pm 0.003 |
| BCE | EfficientNet-B0 | True | 0.521 \pm 0.000 | 0.939 \pm 0.084 |
| Supcon | ResNet18 | False | 1.044 \pm 0.001 | 0.787 \pm 0.088 |
| Supcon | ResNet18 | True | 0.418 \pm 0.000 | 0.716 \pm 0.017 |
| Supcon | ConvNextV2 | True | 0.696 \pm 0.000 | 0.747 \pm 0.055 |
| Supcon [*] | ResNet18 | False | 1.043 \pm 0.002 | 0.995 \pm 0.005 |
| Supcon [*] | ResNet18 | True | 0.418 \pm 0.000 | 0.854 \pm 0.120 |
| Supcon [*] | ConvNextV2 | True | 0.696 \pm 0.000 | 0.823 \pm 0.022 |
| MoCo | ResNet18 | False | 7.367 \pm 0.006 | 0.245 \pm 0.087 |
| SimCLR | ResNet18 | False | 10.872 \pm 0.001 | 0.299 \pm 0.023 |

Table 2: 3D-POP Sequence19 Epoch 10. The asterisk (*) indicates models trained using Supcon with learnable temperature.

| Loss | Network | Train MLP Only | Memory Per Batch (GB) | Accuracy |
|---------------------|-----------------|-------------------|--------------------------|-------------------|
| BCE | ResNet18 | False | 0.871 \pm 0.001 | 0.981 \pm 0.013 |
| BCE | ResNet18 | True | 0.355 \pm 0.000 | 0.891 \pm 0.022 |
| BCE | ConvNextV2 | True | 0.580 \pm 0.000 | 0.902 \pm 0.014 |
| BCE | EfficientNet-B0 | False | 2.791 \pm 0.003 | 0.992 \pm 0.004 |
| BCE | EfficientNet-B0 | True | 0.435 \pm 0.000 | 0.932 \pm 0.001 |
| Supcon | ResNet18 | False | 0.871 \pm 0.000 | 0.978 \pm 0.014 |
| Supcon | ResNet18 | True | 0.355 \pm 0.000 | 0.809 \pm 0.021 |
| Supcon | ConvNextV2 | True | 0.580 \pm 0.001 | 0.823 \pm 0.062 |
| Supcon [*] | ResNet18 | False | 0.872 \pm 0.000 | 0.986 \pm 0.014 |
| Supcon [*] | ResNet18 | True | 0.355 \pm 0.000 | 0.900 \pm 0.022 |
| Supcon [*] | ConvNextV2 | True | 0.580 \pm 0.000 | 0.907 \pm 0.028 |
| MoCo | ResNet18 | False | 7.371 \pm 0.001 | 0.220 \pm 0.049 |
| SimCLR | ResNet18 | False | 10.870 \pm 0.003 | 0.213 \pm 0.009 |

Table 3: 8-calves Epoch 2. The asterisk (*) indicates models trained using Supcon with learnable temperature.

| Dataset | Network | Train MLP Only | Train Frames | Val Frames | Memory Per Batch (GB) | Accuracy |
|-------------------|-----------------|-------------------|-----------------|---------------|--------------------------|----------|
| 3D-POP Sequence11 | EfficientNet-B0 | True | 1000 | 200 | 0.31 | 0.77 |
| 3D-POP Sequence11 | ResNet18 | False | 100 | 100 | 0.66 | 0.88 |
| 3D-POP Sequence11 | ResNet18 | False | 1000 | 200 | 0.66 | 0.96 |
| 3D-POP Sequence19 | EfficientNet-B0 | True | 1000 | 200 | 0.31 | 0.72 |
| 3D-POP Sequence19 | ResNet18 | False | 100 | 100 | 0.66 | 0.89 |
| 3D-POP Sequence19 | ResNet18 | False | 1000 | 200 | 0.66 | 0.97 |
| 8-calves | EfficientNet-B0 | True | 1000 | 200 | 0.27 | 0.61 |
| 8-calves | ResNet18 | False | 100 | 100 | 0.57 | 0.89 |
| 8-calves | ResNet18 | False | 1000 | 200 | 0.57 | 0.96 |

Table 4: Supervised baseline results on 3D-POP and 8-calves datasets.

5 Related Work

The most similar work to ours is the ContrasT[2] paper. It also uses random frame sampling and the application of the Hungarian Algorithm to assign pseudo-labels during training. However, key distinctions arise from our focus on resource efficiency and single-video identification. While ContrasT constructs batches by sampling frames from multiple videos to maximize negative diversity, our method samples frames solely from a single video to minimize computational overhead. Whilst ContrasT requires fine-tuning the entire transformer backbone, ours functions effectively even when fine-tuned with a frozen backbone. And finally, whilst ContrasT employs multiple loss functions to handle joint detection and tracking, ours only requires only a single loss function (SupCon or BCE), and operates on lower-resolution inputs to further lower the GPU memory footprint.

Our loss function design draws inspiration from vision-language models like CLIP and SigLIP, specifically in the use of learnable temperature parameters and the adaptation of Binary Cross Entropy (BCE) for contrastive tasks. The main differences between our method and CLIP and SigLIP are the input modalities and training objectives. CLIP and SigLIP rely on pairing images with text and training from scratch on massive datasets. Our method, conversely, operates purely in the visual domain using image–image pairs for self-supervision and leverages pre-trained weights to bootstrap performance. Additionally, we employ the Hungarian Algorithm to dynamically resolve positive and negative pairs within the batch, a step absent in the static image-text pairing of CLIP and SigLIP.

While standard self-supervised frameworks like SimCLR and MoCo inform our contrastive approach, they are ill-suited for the specific constraints of our domain. These methods typically require training from scratch and rely on large memory banks (as in MoCo) or massive batch sizes with random sampling to learn discriminative features. Our experiments demonstrate that these requirements lead to excessive memory consumption ($>10\text{GB}$) with suboptimal accuracy for animal identification tasks. Our method mitigates this by employing a structured sampling strategy (pairing frames from the same video) rather than random batch sampling, and by utilizing augmentations to double the effective batch size, a feature shared with SimCLR but absent in MoCo’s standard implementation. This allows us to achieve high accuracy with a memory footprint of less than 1GB.

6 Conclusion

We have presented a highly efficient, self-supervised method for identifying individual animals within long-duration video sequences, operating under the practical constraint of a known, fixed population size. By reframing the problem as a global clustering task rather than a sequential tracking problem, our approach eliminates the fundamental issue of error propagation that plagues frame-by-frame association methods, enabling robust performance over extended periods.

The core of our method lies in a memory-conscious design that samples pairs of frames, employs a self-bootstrapping mechanism using the Hungarian algorithm for in-batch pseudo-label assignment, and utilizes a simple yet effective loss function—adapting the Binary Cross Entropy from vision-language models. This design allows us to leverage pre-trained visual backbones effectively, often in a frozen state, reducing the trainable parameters to a lightweight projection head.

Our experiments on challenging real-world datasets (3D-POP pigeons and 8-calves) demonstrate that this minimalist framework achieves state-of-the-art accuracy ($>97\%$), matching or surpassing supervised baselines that require over 1,000 manually annotated frames, while consuming less than 1GB of GPU memory per training batch. This represents an order-of-magnitude reduction in memory compared to standard contrastive learning approaches (SimCLR, MoCo), making high-quality animal identification accessible on consumer-grade hardware.

The key practical outcome is the removal of the manual annotation bottleneck for a common class of wildlife and livestock monitoring scenarios. Researchers can now obtain accurate individual identities from long videos without any labeled data, relying only on pre-existing detections and the prior knowledge of group size.

Future work will focus on extending this framework to more dynamic settings, such as open-world scenarios where the number of individuals is unknown, and on integrating temporal consistency models to further refine features across very long sequences. The principles of resource-efficient,

task-specific self-supervision established here could also benefit other domains where labeled data is scarce and computational resources are limited.

References

- [1] X. Zhai, B. Mustafa, A. Kolesnikov, and L. Beyer, “Sigmoid loss for language image pre-training,” 2023. [Online]. Available: <https://arxiv.org/abs/2303.15343>
- [2] P.-F. D. Plaen, N. Marinello, M. Proesmans, T. Tuytelaars, and L. Van Gool, “Contrastive learning for multi-object tracking with transformers,” in *2024 IEEE/CVF Winter Conference on Applications of Computer Vision (WACV)*. IEEE, Jan. 2024, p. 6853–6863. [Online]. Available: <http://dx.doi.org/10.1109/WACV57701.2024.00672>
- [3] H. Naik, A. H. H. Chan, J. Yang, M. Delacoux, D. I. Couzin, F. Kano, and M. Nagy, “3D-POP—An automated annotation approach to facilitate markerless 2D-3D tracking of freely moving birds with marker-based motion capture,” 2023.
- [4] T. Chen, S. Kornblith, M. Norouzi, and G. Hinton, “A simple framework for contrastive learning of visual representations,” 2020. [Online]. Available: <https://arxiv.org/abs/2002.05709>
- [5] K. He, H. Fan, Y. Wu, S. Xie, and R. Girshick, “Momentum contrast for unsupervised visual representation learning,” 2020. [Online]. Available: <https://arxiv.org/abs/1911.05722>
- [6] A. Radford, J. W. Kim, C. Hallacy, A. Ramesh, G. Goh, S. Agarwal, G. Sastry, A. Askell, P. Mishkin, J. Clark, G. Krueger, and I. Sutskever, “Learning transferable visual models from natural language supervision,” 2021. [Online]. Available: <https://arxiv.org/abs/2103.00020>